

RESEARCH

Open Access



# Transcriptome analysis unveils multiple reasons behind delayed and slower deposition of intramuscular fat compared to subcutaneous fat in cattle

Zhendong Tan<sup>1</sup>, Binod Pokhrel<sup>1</sup>, Ziqi Zhou<sup>1</sup> and Honglin Jiang<sup>1\*</sup>

## Abstract

**Background** Intramuscular fat refers to the white adipose tissue deposited between muscle fibers, and its quantity and distribution directly impact the quality and value of beef. Compared to subcutaneous fat, intramuscular fat develops later and accumulates more slowly in cattle. The reasons for the delayed development and slower growth of intramuscular fat in cattle remain unclear.

**Results** Histological analysis showed that adipocytes in intramuscular fat were smaller than those in subcutaneous fat from the same mature cattle, indicating a delayed development or slower growth of intramuscular fat compared to subcutaneous fat. Intramuscular fat had a lower capacity for retaining or incorporating long-chain fatty acids into triglycerides than subcutaneous fat. Comparing the transcriptomes of intramuscular and subcutaneous fat by RNA sequencing identified more than 1,000 genes differentially expressed (DEGs) between the two adipose depots. Genes upregulated in intramuscular fat included *FOXO6*, *SLC27A1*, *HDAC9*, *WWTR1*, and *PIK3C2A*, which are known to inhibit adipose tissue development and growth. Genes downregulated in intramuscular fat included *FABP4*, *AGPAT2*, *ADIG*, *ADIRF*, and *PLIN2*, which are known to promote adipose tissue development and growth. Functional enrichment analyses of these DEGs suggested that intramuscular fat may have a lower capacity for fatty acid binding and adipogenesis compared to subcutaneous fat. Furthermore, genes downregulated in intramuscular fat were enriched in signaling pathways such as the PPAR signaling pathway, whereas genes upregulated in intramuscular fat were enriched in pathways including the Wnt signaling pathway. Stromal vascular fraction (SVF) cells from intramuscular fat exhibited a lower adipogenic potential than those from subcutaneous fat.

**Conclusions** Multiple factors may contribute to the delayed and slower deposition of intramuscular fat compared to subcutaneous fat in cattle, including reduced fatty acid binding capacity, lower triglyceride synthesis, and decreased adipogenesis in intramuscular fat. These differences are possibly driven by lower expressions of genes such as *AGPAT2*, *FABP4*, and *ADIG*, higher expression of genes such as *FOXO6*, *HDAC9*, and *SLC27A1*, reduced activation of the PPAR signaling pathway, and increased activation of the Wnt signaling pathway in intramuscular fat.

\*Correspondence:

Honglin Jiang  
hojiang@vt.edu

Full list of author information is available at the end of the article



© The Author(s) 2025. **Open Access** This article is licensed under a Creative Commons Attribution-NonCommercial-NoDerivatives 4.0 International License, which permits any non-commercial use, sharing, distribution and reproduction in any medium or format, as long as you give appropriate credit to the original author(s) and the source, provide a link to the Creative Commons licence, and indicate if you modified the licensed material. You do not have permission under this licence to share adapted material derived from this article or parts of it. The images or other third party material in this article are included in the article's Creative Commons licence, unless indicated otherwise in a credit line to the material. If material is not included in the article's Creative Commons licence and your intended use is not permitted by statutory regulation or exceeds the permitted use, you will need to obtain permission directly from the copyright holder. To view a copy of this licence, visit <http://creativecommons.org/licenses/by-nc-nd/4.0/>.

**Keywords** Adipose, Cattle, Intramuscular, Lipid, RNA sequencing, Transcriptome

## Background

White adipose tissue plays an important role in regulating energy homeostasis, storing lipids through lipogenesis during energy surplus and releasing lipids through lipolysis during energy deficiency [1]. Intramuscular fat (IMF) and subcutaneous fat (SF) in cattle are defined as white adipose tissue deposited between the skeletal muscle fibers and beneath the skin, respectively [2]. The deposition of IMF in cattle, also known as marbling, determines the flavor, juiciness, tenderness, and hence the overall quality of beef, and is thus regarded as a highly valuable fat by the meat industry. In contrast, SF is considered less valuable than IMF due to its limited contribution to meat quality [3]. Compared to subcutaneous fat, intramuscular fat develops later and grows more slowly in cattle [4–8]. As such, feeding energy-rich diets during the finishing stage is a common method to increase IMF deposition in cattle and hence the quality and value of beef [9]. However, creating a calorie surplus also increases the deposition of SF and other fat depots. A strategy to enhance IMF deposition without increasing the deposition of SF or other less-valuable fat depots in cattle would be more attractive than feeding cattle energy-rich diets. Developing such a strategy requires a better understanding of why IMF develops later and grows more slowly than SF or other fat depots in cattle.

Adipocytes are formed from adipose progenitor cells (APCs) or mesenchymal stem cells (MSCs) [10]. Adipogenesis involves the sequential steps of commitment of APCs or MSCs to preadipocytes, proliferation of preadipocytes, and terminal differentiation of preadipocytes into adipocytes [11, 12]. Multiple proteins control the adipogenic commitment in APCs, including bone morphogenetic protein 2 (BMP2) and BMP4 that activate the SMAD family member 4 (SMAD4) transcription factor and subsequently induce the expression of peroxisome proliferator-activated receptor-gamma (*PPARG*) gene [13]. The transcription factor zinc finger protein 423 (ZFP423) is preferentially expressed in adipogenic fibroblasts and sensitizes these cells to pro-adipogenic BMP signaling [14]. Kruppel-like factor 5 (KLF5) serves as a co-activator of CCAAT/enhancer-binding protein beta (CEBPB), which promotes the transcription of *PPARG* and *CEBPA* [15]. Conversely, transcription factors such as GATA binding protein 2 (GATA2) and GATA3 and the transcriptional co-repressor RUNX1 partner transcriptional co-repressor 1 (RUNX1T1) inhibit adipogenesis by preventing *PPARG* transcription [16, 17]. The proliferation of preadipocytes is controlled by various hormones such as leptin [18], growth hormone [19], androgens, and estrogens [20]. The differentiation of preadipocytes into

adipocytes is chiefly controlled by the *PPARG* and *CEBP* families of transcription factors [21]. The growth of adipocytes is controlled by lipogenesis and lipolysis, which are both controlled by nutrition and hormones [22, 23].

IMF preferentially utilizes glucose as a substrate for fatty acid synthesis, whereas SF primarily synthesizes fatty acids from acetate, which is a more abundant energy source than glucose in cattle and other ruminants [24]. IMF exhibits a lower lipogenic rate than SF [25, 26], and several genes involved in fatty acid synthesis are expressed at lower levels in IMF than in SF [27, 28]. These findings suggest that the delayed and slower deposition of IMF compared to SF in cattle may be due to more limited fatty acid synthesis in IMF. Despite these significant findings, we hypothesized that additional mechanisms contribute to the delayed development and slower growth of IMF compared to SF in cattle. These mechanisms may include reduced preadipocyte proliferation or differentiation, decreased fatty acid uptake, or lower triglyceride synthesis in IMF relative to SF. Because IMF is tightly associated with muscle fibers, preadipocyte proliferation and differentiation, fatty acid uptake, and triglyceride synthesis in IMF may be more restricted by muscle-derived factors than in SF. All these possibilities can be investigated by comparing gene expression profiles between IMF and SF and the subsequent functional analyses. Therefore, the primary objective of this study was to compare the transcriptomic profiles of IMF and SF in adult cattle.

## Methods

### Animals and sample collection

The *longissimus dorsi* muscle (~100 g) for intramuscular fat isolation and subcutaneous fat tissue (~10 g) were collected between the 6th and 7th ribs from finished Angus-crossbred heifers (around 18 months old) at slaughter. These animals were fed a high-energy diet composed of grain and silage to promote rapid weight gain and fat deposition during the 6 months prior to slaughter. From the muscle samples, visible IMF tissues were carefully dissected out from between muscle fibers (not from between muscle bundles), and any visible muscle tissues attached to IMF were carefully removed with scissors. Adipose tissue samples for RNA extraction were immediately immersed in liquid nitrogen and stored at -80 °C until further analysis. Adipose tissue samples for histology were fixed in 10% phosphate-buffered formalin (Sigma-Aldrich, St. Louis, MO, USA). Adipose tissue samples for cell isolation were transported on ice in phosphate-buffered saline (PBS) to the laboratory for further processing (see below) within four hours of collection.

### Histological examination

Tissue samples were fixed in 10% formalin for 72 h and subsequently stored in 70% ethanol at 4 °C until further processing. The fixed tissue samples underwent a dehydration process, transitioning through 70% ethanol for 1 h, 80% ethanol for 1 h, 95% ethanol for 1 h (repeated twice), and finally, 100% ethanol for 1 h (repeated twice). Subsequently, the samples were treated with xylene for 1 h (repeated twice) before being embedded in paraffin. The embedded tissue blocks were sectioned into 10 µm-thick slices using an Eprelia HM 340E Electronic Rotary Microtome (ThermoFisher Scientific, Waltham, MA, USA) and subsequently stained with hematoxylin and eosin (H&E, Sigma-Aldrich). Briefly, tissue slides were first subjected to four rounds of xylene incubation (20 s each) for deparaffinization and then two rounds of 100% ethanol incubation (20 s each). Subsequently, tissue slides were incubated in 95% ethanol for 15 s, stained with H&E (15 s each), and dehydrated in the increasing concentrations of ethanol. Images of three randomly selected areas were obtained from each section with a Nikon ECLIPSE 80i microscope (Nikon Corporation, Tokyo, Japan). The areas of all adipocytes within each image were determined using the ImageJ program [29]. On average, around 2000 adipocytes were counted for each adipose tissue sample.

### Lipid uptake and accumulation assays

Fresh intramuscular and subcutaneous adipose tissue samples collected from the same animals were cut into approximately 1 mm-thick slices in PBS. The adipose tissue slices were then transferred to DMEM/F12 medium (ThermoFisher Scientific) containing 5 µM BODIPY FL C16, a fluorescently labeled palmitic acid analog (ThermoFisher Scientific) in a six-well culture plate. An inverted cell strainer was used to ensure the adipose tissue explants were fully immersed in the culture medium. The adipose tissue explants were incubated with BODIPY FL C16 in a 37 °C incubator supplied with 5% CO<sub>2</sub> for 10 min–4 h. The 10-minute incubation was used to measure lipid uptake, based on the previous finding that the uptake of BODIPY fatty acids by tissue explants and cells stabilized within 15 min [30]. The 4-hour incubation was used to measure long-term accumulation of BODIPY FL C16 in adipose explants. Following the incubation, the adipose tissue explants were washed 3 times with PBS and homogenized in 1 mL chloroform/methanol (1:2 v/v). The homogenates were centrifuged at 500 g for 10 min. One hundred µL of the organic phase were transferred to a 96-well plate, and fluorescence was measured using a Tecan Infinite 200 PRO microplate reader (Tecan Group Ltd., Männedorf, Switzerland) at an excitation wavelength of 500 nm and an emission wavelength of 510 nm. Fluorescence from each incubation was measured in

triplicate. The fluorescence intensity measured from each incubation was normalized to the mass of the adipose tissue used in the incubation.

### RNA sequencing and bioinformatic analyses

Total RNA was extracted using the Direct-zol RNA Mini-Prep Plus Kit (Zymo Research, Irvine, CA, USA) following the manufacturer's instructions. RNA concentrations were quantified using a NanoDrop One spectrophotometer (ThermoFisher Scientific, Waltham, MA, USA). RNA quality assessment and RNA sequencing (RNA-seq) library construction were performed by Novogene Corporation (Sacramento, CA, USA). All ten RNA samples for RNA-seq had an RNA integrity number (RIN) greater than 7. Non-stranded RNA-seq libraries were generated using the mRNA-Seq Library Preparation V2 Kit (ABclonal, Woburn, MA, USA). The RNA-seq libraries were pooled and paired-end sequenced on an Illumina NovaSeq 6000 platform.

Low quality sequencing reads and reads containing adapters were removed using Trimmomatic v0.39 [31]. Clean reads were mapped to the reference bovine genome *Bos taurus* ARS-UCD2.0 using HISTA2 [32]. Gffread v0.12.18 was used to convert the genomic annotation files from gff to gtf format [33]. Gene expression quantification was performed using FeatureCounts (v2.0.2) [34]. Genes with less than 20 total read counts across all samples were removed from further analyses. Gene expression was calculated as transcripts per million (TPM). Differential gene expression analysis was performed using DESeq2 (v1.43.1) in R [35]. Genes with Benjamin-Hochberg adjusted *p*-values < 0.05 and |log<sub>2</sub>fold change| ≥ 1 were designated as differentially expressed genes (DEGs). Genes upregulated in IMF compared to SF were submitted to the STRING v12.0 database to identify known and predicted protein-protein interactions (PPIs). The resulting interaction network was visualized and analyzed in Cytoscape [36]. The MCODE plugin in Cytoscape was utilized to reveal significant sub-networks or clusters of genes within the imported network. The clustering parameters used were as follows: degree cut-off = 2, node score cut-off = 0.2, K-score = 5, and maximum depth = 100. Genes specific to skeletal muscle were omitted from further analysis as these genes likely reflected the incomplete removal of skeletal muscle tissue from intramuscular fat. After excluding the skeletal muscle-specific genes from the gene list, differential expression analysis was performed again. Gene ontology (GO) and KEGG pathway analyses were performed using the ClusterProfiler (v4.10.0) R package [37].

### Isolation and culture of stromal vascular fraction (SVF) cells from adipose tissue

Subcutaneous and intramuscular adipose tissue samples freshly collected from the same animals were washed three times with PBS and then cut into pieces of approximately 1 mm<sup>3</sup>. Adipose tissue pieces were digested with type I collagenase (ThermoFisher Scientific) at a concentration of 2 mg/mL for 1 h at 37 °C. The dissociated cells were filtered through a 100 µm cell strainer, and the filtrates were centrifuged at 500 g for 15 min at room temperature. After centrifugation, the cell pellet was resuspended and incubated with 1× red blood cell lysis buffer (ThermoFisher Scientific) at room temperature for 5 min to remove red blood cells. Following another centrifugation, the SVF cells were either cryopreserved or cultured in growth medium consisting of DMEM, 10% fetal bovine serum (FBS) (Atlanta Biologicals, Lawrenceville, GA, USA), 1% antibiotics–antimycotics (ABAM), and 2 mM L-glutamine (ThermoFisher Scientific) at 37 °C and under 5% CO<sub>2</sub>. The medium was changed every 3 days.

To be differentiated into adipocytes, the SVF cells were cultured in the growth medium for 2 more days after reaching confluency and then cultured for 2 days in differentiation medium consisting of DMEM/F12, 10 µg/mL bovine insulin (Sigma-Aldrich), 0.25 µM dexamethasone (Sigma-Aldrich), 0.5 mM 3-isobutyl-1-methylxanthine (IBMX, Sigma-Aldrich), and 1 µM rosiglitazone (Cayman Chemical, Ann Arbor, MI, USA). Subsequently, the cells were cultured in maintenance medium consisting of DMEM/F12, 10 µg/mL insulin, and 1 µM rosiglitazone for 4 days before Oil Red O staining or RNA extraction.

### Cell proliferation assay

Approximately 5000 SVF cells per well were seeded in 96-well plates and cultured in growth medium for 24, 48, 72, or 96 h. Eight wells were used for SVF cells from each animal. The number of viable cells was quantified using a Cell Counting Kit-8 (CCK-8) assay kit (GlpBio, Montclair, CA, USA), following the manufacturer's instructions. In brief, 10 µL CCK-8 solution was added to each well, and the plate was then incubated at 37 °C for 4 h in a CO<sub>2</sub> incubator. Absorbance at 450 nm was measured using a PowerWave 340 microplate reader (BioTek Instruments, Winooski, VT, USA).

### Oil Red O staining

Cells were washed twice with PBS and then fixed in 10% neutral buffered formalin (Sigma-Aldrich) at room temperature for 1 h. After fixation, cells were washed twice with PBS and subsequently stained with 3.5 mg/mL Oil Red O in 60% isopropanol (ThermoFisher Scientific) for 15 min. Cells were then rinsed with water and photographed using an OLYMPUS DP74 color digital camera

and an OLYMPUS CKX41 inverted microscope (Olympus Corporation, Tokyo, Japan). For quantitative analysis, we extracted Oil Red O from cells with 100% isopropanol and measured the absorbance of extracted Oil Red O at a wavelength of 500 nm. Following Oil Red O quantification, we stained the cells with 300 nM 4',6-diamidino-2-phenylindole (DAPI) for 10 min, washed the cells three times with PBS, and then lysed the cells with 1 mL of 2% sodium dodecyl sulfate (SDS). DAPI in the cell lysates was quantified by measuring the fluorescence intensity at an excitation wavelength of 370 nm and an emission wavelength of 460 nm as described previously [38]. The absorbance of Oil Red O was divided by the fluorescence intensity of DAPI in the same well to control for variation in cell number.

### Total RNA extraction and reverse transcription-quantitative PCR

cDNA was synthesized using random primers and the ImProm-II reverse transcription system (Promega, Madison, Wisconsin, USA), according to the manufacturer's protocol. Quantitative PCR (qPCR) was performed in duplicate using the Power SYBR Green PCR Fast Master Mix (Applied Biosystems, Foster City, CA, USA) on an Applied Biosystems 7500 Real-time PCR System. The PCR conditions were as follows: an initial denaturation at 95 °C for 20 s, followed by 40 cycles of denaturation at 95 °C for 3 s and annealing/extension at 60 °C for 30 s. The sequences of primers used in qPCR are provided in Table 1. qPCR data were analyzed using the 2<sup>−(ΔΔCt)</sup> method [39], with the HMBS gene as the internal control. Based on the Ct values, HMBS mRNA expression was not different between the conditions used in this study (data not shown).

### Statistical analysis

Statistical analysis was performed using JMP Pro v16.0.0 (SAS, Cary, NC, USA). Data from two groups (IMF vs. SF) were analyzed by Student's t-test. Data from multiple groups (the data in Fig. 6D and E) were analyzed by one-way ANOVA, with individual animals included as a blocking factor in the model to account for individual variation, followed by Tukey's test. All data are expressed as mean ± SEM, with *n* = 5 for the RNA-seq data and *n* = 6 for the other data. Differences were considered significant at *P* < 0.05.

## Results

### Mature adipocytes in intramuscular fat were smaller than those in subcutaneous fat

We first performed a histological analysis to compare the size of adipocytes in IMF and SF collected from the same cattle. This histological analysis showed significant differences in the size of mature adipocytes between IMF and

**Table 1** The sequences of PCR primers used in this study

Gene ID	Primer sequence*	GenBank accession number	Product size
HMBS	F: CTTTGGAGAGGAATGAAGTGG R: AATGGTGAAGCCAGGAGGAA	NM_001046207.1	80
PPARG	F: CAGTGTCTGCAAGGACCTCA R: ATAGTGCAGAGTGGAAATGC	NM_181024.2	176
CEBPA	F: ATCGACATCAGCGCTACAT R: CGGGTAGTCAAAGTCGTTGC	NM_176784.2	138
FABP4	F: AATTGGGCCAGGAATTTGAT R: TGGTGGTTGATTTCCATCC	NM_174314.2	117
ADIPOQ	F: AGGTTGGATGGCAGGCATT R: GGACCTTCGATCCCAGTGATT	XM_024995232.2	162
LEP	F: GACATCTCACACGCAGTC R: ATCGCCAATGTCTGGTCCAT	NM_173928.2	113
DGAT1	F: CTTCAGCAACTACCGTGCCA R: GGCAAAGATATTGGCCACAATGA	NM_174693.2	190
DGAT2	F: CAGCTCCAAGTCATCTCGGT R: TGACCTCTGCCACCTTTCTT	NM_205793.2	174
TMEM68	F: AATCGGAAAGGCTTCGCTCA R: AGCCACCTAAACAGCCTTGT	NM_001076009.1	119
FOXO6	F: GTCGGTACGTGCCCTACTT R: ACCAGGAAGCTTTCGCTGTG	XM_024990211.2	139
PIK3C2A	F: GGTGCTTTAGATGGCGTGGA R: TCAGGATTCAGTGAGCCCCTA	XM_024975781.2	158
NOCT	F: GAACATCTTGCCCAAGCTCT R: TAGGCGAGGATCTCCTCCAG	NM_001082454.2	114
ARHGAP24	F: TGTTTGTGCAAGGAGGCGAT R: CCAGGCGGTTCCCATATCTC	NM_001102234.1	198
SLC27A1	F: CCAACGCACTGTACGAGGA R: CTTCTGAATTTTGAAGGTGCCTGT	NM_001033625.2	110
ADIG	F: CTGAGCCTATTCTGCCTGATTC R: GTGTCCATCAGTGGAGGAGC	NM_001113720.2	175
PLIN5	F: ACCTTCGAGACGGTGGTGA R: ATGGCATGGCTCACAGATCG	NM_001101136.1	126
PLIN2	F: GCGTCTGCTGGCTGATTTCT R: TGTAAGCCGAGGAGACCAAGA	NM_173980.2	139
ADIRF	F: GCTACCTTAACCACTCGCA R: AACCTGGTCCATGGCTTTCT	NM_001114513.2	172
AGPAT2	F: CCATGAGCGTGATGACCGAT R: CAGGGATGATGGGTACCTGG	NM_001080264.1	159

\*F: forward; R: reverse

SF in adult cattle (Fig. 1A). Specifically, the average size of mature adipocytes in IMF was 25% smaller than that in SF (Fig. 1B,  $P < 0.05$ ,  $n = 6$ ), and IMF had a higher density of smaller adipocytes compared to SF (Fig. 1C).

#### Intramuscular fat had a lower ability to incorporate long-chain fatty acids into triglyceride or to retain them compared to subcutaneous fat

We next compared the ability of IMF and SF collected from the same cattle to take up long-chain fatty acids and incorporate them into triglyceride or to retain them. Following a 10 min-incubation with a fluorescently labeled

palmitate analog BODIPY FL C16, no difference was observed in the amounts of BODIPY FL C16 accumulated in the explants of IMF and SF ( $P = 0.45$ ,  $n = 6$ , Fig. 2A), indicating that the two types of fat did not differ in the ability to take up long-chain fatty acids. However, following a 4-hour incubation with BODIPY FL C16, the IMF explants accumulated 35% less fluorescence than the SF explants ( $P < 0.01$ ,  $n = 6$ , Fig. 2B), indicating that IMF had a lower ability to incorporate long-chain fatty acids into triglyceride or that IMF had a lower ability to retain long-chain fatty acids than did SF.

#### Intramuscular fat and subcutaneous fat differed in gene expression profile

We next compared the gene expression profiles between IMF and SF by RNA-seq. RNA-seq libraries were prepared from IMF and SF samples taken from the same five cattle. Sequencing these RNA-seq libraries generated approximately 476 million high-quality reads, ranging from 41.7 million to 53.4 million per library (Supplementary Table 1). On average, 89.9% (ranging from 87.0 to 90.2%) of these reads aligned uniquely to the bovine genome (Supplementary Table 1).

Based on a principal component analysis (PCA), the gene expression profiles of five IMF samples clustered separately from those of five SF samples (Fig. 3A). Based on a differential expression analysis, 1,191 DEGs (adjusted  $P < 0.05$ ,  $|\log_2\text{FoldChange}| \geq 1$ ) were identified between IMF and SF, comprising 359 downregulated and 832 upregulated genes in IMF compared to SF (Fig. 3B and C). Based on fold change, the top 10 genes expressed at higher levels in IMF than SF included *NMRK2*, *ENSBTAG00000052709*, *SYNPO2L*, *GADLI*, *ANO5*, *CACNG6*, *LRRC30*, *NEFM*, *CACNA2D2*, and *NT5C1A* (Table 2), and the top 10 genes expressed at lower levels in IMF than SF included *HMX1*, *DMRT3*, *TBX4*, *CYP17A1*, *CHST9*, *ACR*, *TF*, *EPHA10*, *LAMC3*, and *NPB* (Table 3). The complete lists of DEGs are shown in Supplementary Table 2.

Several genes known to inhibit adipose tissue development and growth were upregulated (adjusted  $P < 0.05$ ,  $|\log_2\text{FoldChange}| \geq 1$ ) in IMF compared to SF (Table 4), including *FOXO6*, *SLC27A1*, *HDAC9*, *WWTR1*, and *PIK3C2A*. Several genes known to stimulate adipose tissue development and growth were downregulated (adjusted  $P < 0.05$ ,  $|\log_2\text{FoldChange}| \geq 1$ ) in IMF compared to SF (Table 4), including *FABP4*, *AGPAT2*, *ADIG*, *ADIRF*, and *PLIN2* and *PLIN5*. In addition to these genes, genes *PPARG*, *DGAT1*, *PLIN4* and *FASN*, which are associated with adipogenesis [40], triglyceride synthesis [41], maintenance of lipid droplets [42], and fatty acid synthesis [43], respectively, were also expressed at lower levels in IMF than in SF (adjusted  $P < 0.05$ ), although these differences were not greater than twofold (Supplemental

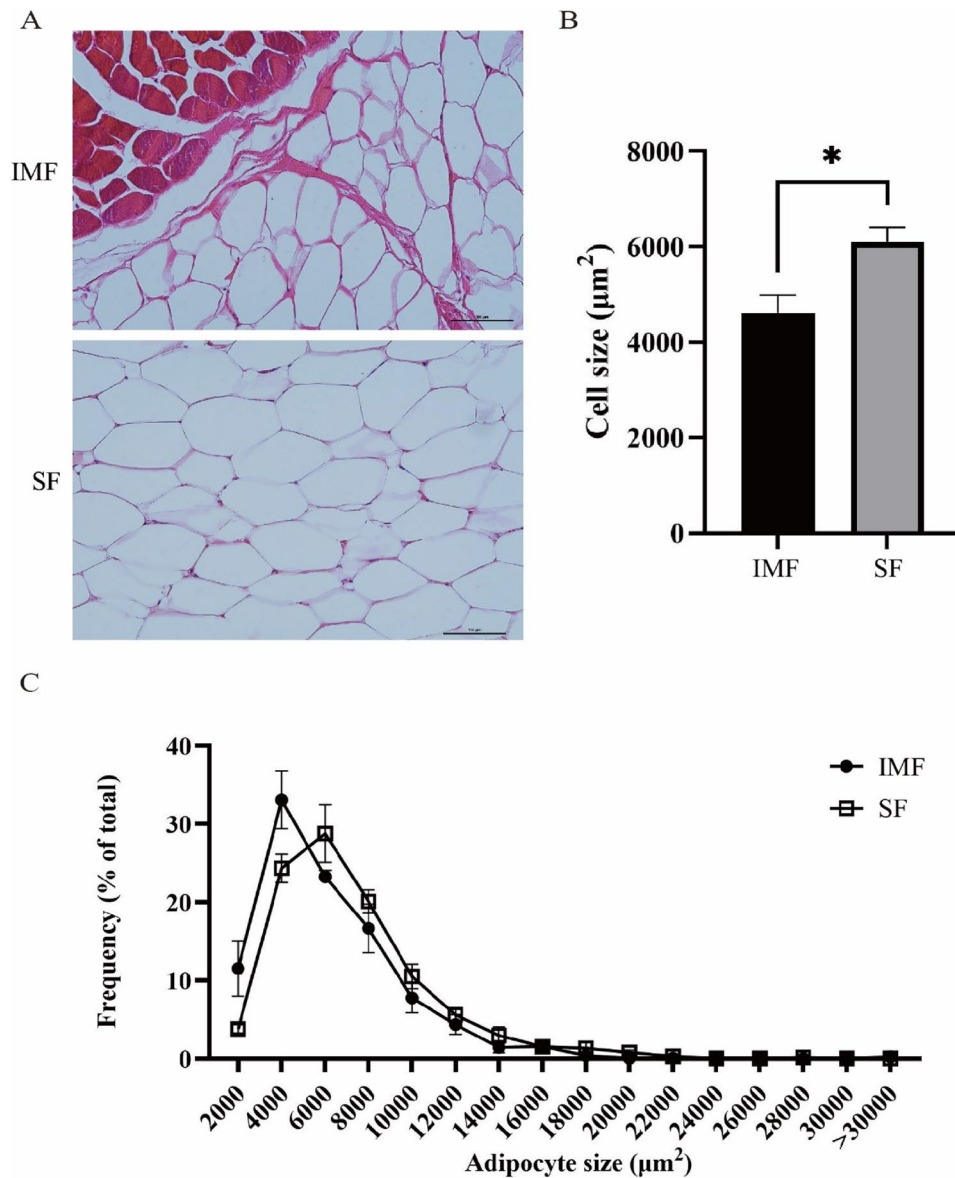


**Fig. 1** Histological analysis of adipocytes in bovine intramuscular fat (IMF) and subcutaneous fat (SF). **A** Hematoxylin and eosin staining of sections of IMF and SF. Scale bar: 100  $\mu\text{m}$ . **B** Average size of adipocytes in IMF and SF. \* $P < 0.05$  ( $n = 6$ ). **C** Size distribution of adipocytes in IMF and SF

Table 2). To validate the RNA-seq results, we selected 11 genes and quantified their expression in the same IMF and SF RNA samples used for RNA-seq by RT-qPCR. As shown in Fig. 4, all these genes were confirmed to be differentially expressed between IMF and SF by RT-qPCR.

#### Genes downregulated in intramuscular fat compared to subcutaneous fat were enriched in fatty acid binding, fatty acid synthesis, and PPAR signaling

Gene Ontology (GO) enrichment analyses of genes upregulated in IMF compared to SF revealed 271 significantly enriched terms ( $P < 0.05$ , Supplementary Table 3). Among these GO terms, 198 represented biological processes, including insulin receptor signaling pathway,

response to glucocorticoid, adult locomotory behavior, and regulation of microtubule polymerization; 40 represented cellular components, including external encapsulating structure, extracellular matrix, axon, and presynapse; and 34 represented molecular functions, including calcium ion binding, gated channel activity, monoatomic ion gated channel activity, and ATPase regulator activity (Fig. 5A).

Gene Ontology enrichment analyses of genes downregulated in IMF compared to SF identified 205 significantly enriched GO terms ( $P < 0.05$ , Supplementary Table 4). Among these were 177 biological processes, including monocarboxylic acid metabolic process, fatty acid metabolic process, lipid metabolic process, and long-chain

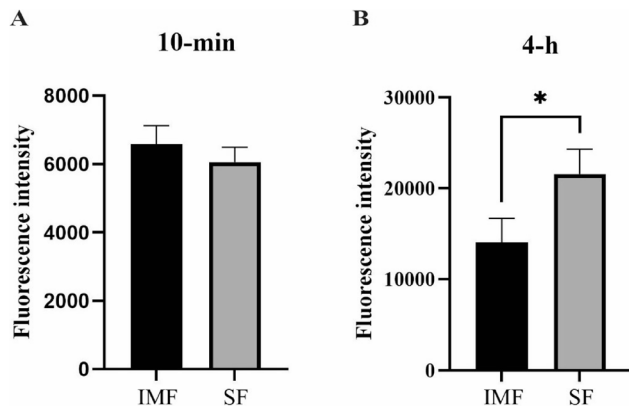


**Fig. 2** Comparing long-chain fatty acid uptake and accumulation between intramuscular fat (IMF) and subcutaneous fat (SF). Long-chain fatty acid uptake and accumulation were measured by incubating adipose tissue explants with fluorescently labeled palmitic acid analog BODIPY FL C16 for 10 min and 4 h, respectively. **A** Relative amount of BODIPY FL C16 accumulated in adipose tissue explants following 10-min incubation. **B** Relative amount of BODIPY FL C16 accumulated in adipose tissue explants following 4-h incubation. \* $P < 0.05$  ( $n = 6$ )

fatty acid metabolic process; 12 cellular components, including extracellular region, extracellular space, extracellular vesicle, and extracellular organelle; and 16 molecular functions, including monocarboxylic acid binding, lipid binding, fatty acid binding, and carboxylic acid binding (Fig. 5B).

Pathway enrichment analyses revealed 65 KEGG pathways associated with genes upregulated in IMF compared to SF ( $P < 0.05$ , Supplementary Table 5), including the endocrine system and signal transduction, the oxytocin signaling pathway, the cGMP-PKG signaling pathway, the MAPK signaling pathway, and the Wnt signaling pathway (Fig. 5C). Pathway enrichment analyses identified 39 KEGG pathways associated with genes downregulated in IMF compared to SF ( $P < 0.05$ , Supplementary Table 6), including diseases and metabolism, the PPAR signaling pathway, cholesterol metabolism, fatty acid biosynthesis, and fatty acid metabolism (Fig. 5D).

Overall, these functional enrichment analyses indicated that genes associated with fatty acid binding, fatty acid synthesis, and the PPAR signaling pathway were significantly downregulated, whereas those associated with the insulin receptor, MAPK, and Wnt signaling pathways were significantly upregulated in IMF compared to SF.

#### The stromal vascular fractions of intramuscular fat and subcutaneous fat did not differ in cell proliferation, but the former had a lower adipogenic potential than the latter

The RNA-seq data described above indicated that IMF has a lower adipogenic potential than SF. To validate this functional difference, we isolated SVF cells from IMF and SF and compared their proliferation rates in vitro. Based on a CCK-8 assay, the SVF cells of IMF and SF showed no

difference in the rate of proliferation during a 4-day culture ( $P = 0.55$ ,  $n = 6$ , Fig. 6A). We also compared the ability of these cells to differentiate into adipocytes. Based on Oil Red O staining (Fig. 6B) and subsequent quantification, the IMF SVF cells accumulated 33.6% less lipid than the SF SVF cells by day 6 of induced adipogenic differentiation ( $P < 0.01$ ,  $n = 6$ , Fig. 6C). Gene expression analyses showed that 7 markers of differentiated adipocytes, including *CEBPA*, *PPARG*, *FABP4*, *LEP*, *ADIPOQ*, *DGAT2*, and *TMEM68*, were expressed at much higher levels in both the IMF and SF SVF cells on day 6 of adipogenic differentiation ( $P < 0.05$ ,  $n = 6$ , Fig. 6D and E), confirming the differentiation of these SVF cells into adipocytes. Gene expression analyses also showed that 6 of these genes, including *CEBPA*, *PPARG*, *FABP4*, *ADIPOQ*, *DGAT1*, and *DGAT2*, were expressed at lower levels in the IMF SVF cells than in the SF SVF cells on day 6 of adipogenic differentiation ( $P < 0.05$ ,  $n = 6$ , Fig. 6D and E). These gene expression data, along with the Oil Red O data, indicated that the IMF SVF cells had a lower adipogenic potential than the SF SVF cells.

#### Discussion

Previous research comparing IMF and SF focused on the influence of different cattle breeds and feed structures on fatty acid composition [44–46], and these studies did not directly explain the differences in growth and development between these adipose tissues. In this study, by comparing the gene expression profiles of IMF and SF, we found that more than 1,000 genes were differentially expressed between the two fat depots. Examples of genes upregulated in IMF compared to SF were *FOXO6*, *SLC27A1*, *HDAC9*, *WWTR1*, and *PIK3C2A*. All these genes are known to play a negative role in adipose tissue development and growth. *FOXO6* inhibits both the proliferation and differentiation of preadipocytes by upregulating cyclin G2, a cell cycle inhibitor, and by suppressing the expression of *PPARG* and *CEBPA* genes, two master transcriptional regulators of adipogenesis [47]. *SLC27A1* encodes a fatty acid transport protein (FATP1) involved in the uptake and utilization of long-chain fatty acids [48], and its expression is negatively correlated with adipocyte size [49]. Overexpression of *SLC27A1* enhanced fatty acid oxidation and reduces triglyceride accumulation, whereas knockdown of *SLC27A1* impaired lipid metabolism [50]. *HDAC9* encodes a class II histone deacetylase; its overexpression inhibits the differentiation whereas its deletion restores the adipogenic potential of preadipocytes [51]. *WWTR1* (also known as *TAZ*) functions as a co-repressor of *PPARG* in adipose tissue, suppressing the expression of adipogenesis-related genes; adipocyte-specific deletion of *WWTR1* enhances *PPARG* activity and increases the expression of adipogenic

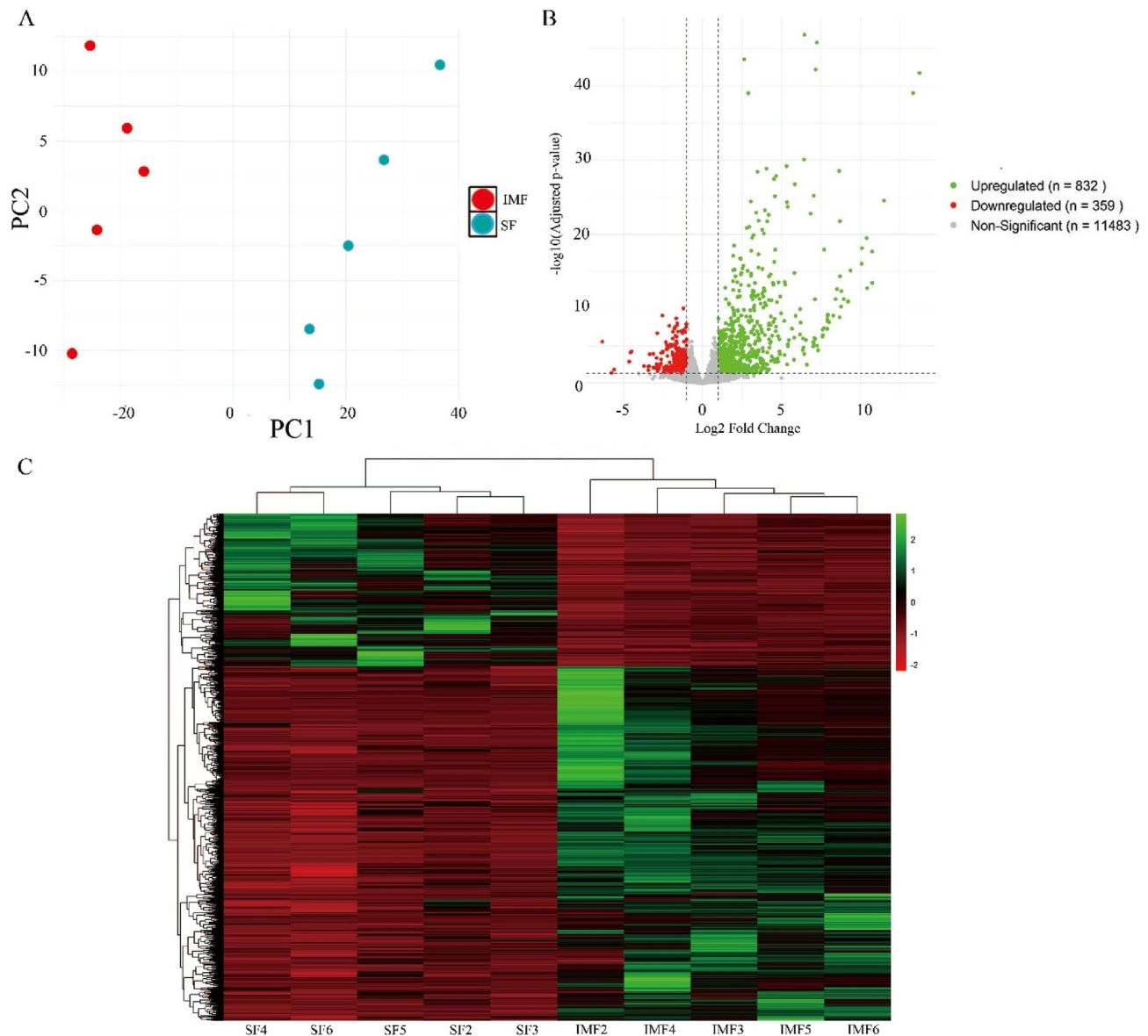


**Fig. 3** Transcriptomic analysis of intramuscular fat (IMF) and subcutaneous fat (SF) by RNA sequencing. **A** Principal component (PC) analysis. Note that the gene expression profiles from 5 IMF samples and 5 SF samples are well separated on PC1. **B** Volcano plot of genes upregulated and downregulated (adjusted  $P < 0.05$ ,  $|\log_2\text{Fold change}| \geq 1$ ) in IMF compared to their expression in SF. **C** Heatmap showing the expression levels and clustering of genes differentially expressed between IMF and SF. Each row represents a gene and each column represents a tissue sample. Green color indicates genes with high expression levels; red color indicates genes with low expression levels; and the gradient between these colors reflects the range of gene expression levels from high to low

markers [52]. Systemic inactivation of PI3K-C2 $\alpha$ , which is encoded by the *PI3KC2A* gene, in mice led to age-dependent obesity and adipocyte hypertrophy, suggesting that *PI3KC2A* may function to restrain excessive fat accumulation under physiological conditions [53]. Collectively, the higher expression of these genes in IMF than in SF may contribute to the slower differentiation and growth of IMF compared to SF.

Among the genes downregulated in IMF compared to SF were *AGPAT2*, *FABP4*, *ADIG*, *ADIRE*, *PLIN2*, and *PLIN5*. The *AGPAT2* gene, which converts

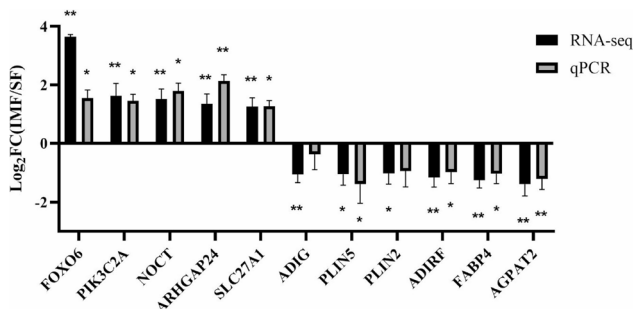
lysophosphatidic acid to phosphatidic acid in the second step of *de novo* phospholipid biosynthesis, is essential for the development and growth of adipose tissue. The *agpat2*-deficient mice exhibit lipodystrophy, highlighting the critical role of this gene in adipose tissue formation [54]. A recent study further demonstrated that *Agpat2*<sup>-/-</sup> preadipocytes fail to undergo adipogenic differentiation in vitro, exhibiting markedly reduced lipid accumulation and expression of adipocyte markers, despite no evidence of excessive apoptosis or autophagic failure. These findings further indicate that *AGPAT2* is

**Table 2** Top 10 upregulated genes in intramuscular fat (IMF) compared to subcutaneous fat (SF)

Gene ID	Log2FC (IMF/SF)	$P_{adj}$ -value	Gene description
NMRK2	13.7	0.001	Nicotinamide riboside kinase 2
ENSBTAG00000052709	13.3	0.001	N/A
SYNPO2L	11.5	0.001	Synaptopodin 2 like
GADL1	10.7	0.001	Glutamate decarboxylase like 1
ANO5	10.7	0.001	Anoctamin 5
CACNG6	10.4	0.001	Calcium voltage-gated channel auxiliary subunit gamma 6
LRR30	10.4	0.001	Leucine rich repeat containing 30
NEFM	10.0	0.001	Neurofilament medium
CACNA2D2	10.1	0.001	Calcium voltage-gated channel auxiliary subunit alpha2delta 2
NT5C1A	9.4	0.001	5'-nucleotidase, cytosolic IA

**Table 3** Top 10 downregulated genes in intramuscular fat compared to subcutaneous fat

Gene ID	Log2FC (IMF/SF)	$P_{adj}$ -value	Gene description
HMX1	-6.3	0.001	H6 family homeobox 1
DMRT3	-5.7	0.008	Doublesex and mab-3 related transcription factor 3
TBX4	-5.5	0.002	T-box 4
CYP17A1	-4.6	0.001	Steroid 17-alpha-hydroxylase/17,20 lyase
CHST9	-4.5	0.001	Carbohydrate sulfotransferase 9
ACR	-4.4	0.001	Acrosin
TF	-3.7	0.001	Transferrin
EPHA10	-3.4	0.002	EPH receptor A10
LAMC3	-3.4	0.001	Laminin subunit gamma 3
NPB	-3.3	0.001	Neuropeptide B

**Fig. 4** RT-qPCR validation of log2 fold changes of selected genes between IMF and SF determined by RNA-seq. \* $P < 0.05$ ; \*\* $P < 0.01$  ( $n = 5$ )**Table 4** Differential expression of genes involved in adipose tissue development and growth between intramuscular fat and subcutaneous fat

Gene ID	Log2FC (IMF/SF)	$P_{adj}$ -value	Gene description
FOXO6	3.6	0.01	Forkhead box O6
HDAC9	2.3	0.01	Histone Deacetylase 9
PIK3C2A	1.6	0.01	Phosphatidylinositol-4-phosphate 3-kinase catalytic subunit type 2 alpha
WWTR1	1.4	0.01	WW Domain Containing Transcription Regulator 1
SLC27A1	1.3	0.01	Solute carrier family 27 member 1
ADIG	-1.0	0.01	Adipogenin
PLIN5	-1.0	0.03	Perilipin 5
PLIN2	-1.0	0.03	Perilipin 2
ADIRF	-1.1	0.01	Adipogenesis regulatory factor
FABP4	-1.2	0.01	Fatty acid binding protein 4
AGPAT2	-1.3	0.01	1-acylglycerol-3-phosphate O-acyltransferase 2

directly required for the adipogenic program independent of the cell survival pathways [55]. FABP4, an adipocyte-type fatty acid binding protein, plays a positive role in fatty acid uptake and transport in adipocytes. It facilitates the intracellular transport of lipids to biological targets and signaling pathways, contributing to adipocyte function and lipid metabolism [56–58], and it also functions as a vital auxiliary factor in terminal adipocyte differentiation [59]. Live single-cell imaging studies have shown that preadipocytes only commit to terminal differentiation after upregulation of *FABP4*, which engages a positive feedback loop with *PPARG* [59]. The *ADIG* gene is another gene essential for adipocyte differentiation, as its deficiency impairs adipogenesis in cultured cells and reduces fat mass in mice when fed a high-fat diet [60]. The *ADIRF* protein promotes adipocyte differentiation and plays a role in initiating early events of adipogenesis [61, 62]. The *PLIN* family proteins (e.g., *PLIN2* and *PLIN5*) constitute the amphiphilic interface between lipids and cytoplasm, protecting lipid droplets against lipase [63, 64]. *PLIN2* is highly expressed during the early stages of adipocyte differentiation and plays a critical role in lipid droplet formation and stability [65]. *PLIN5* promotes triglyceride storage and suppresses fatty acid  $\beta$ -oxidation, making it essential for adipocyte maturation and lipid homeostasis [66]. Because *AGPAT2*, *FABP4*, *ADIG*, *ADIRF*, *PLIN2*, and *PLIN5* regulate key aspects of adipocyte differentiation, lipid metabolism, and droplet stability, their reduced expression in IMF compared to SF may contribute to the delayed development and slower growth of IMF compared to SF.

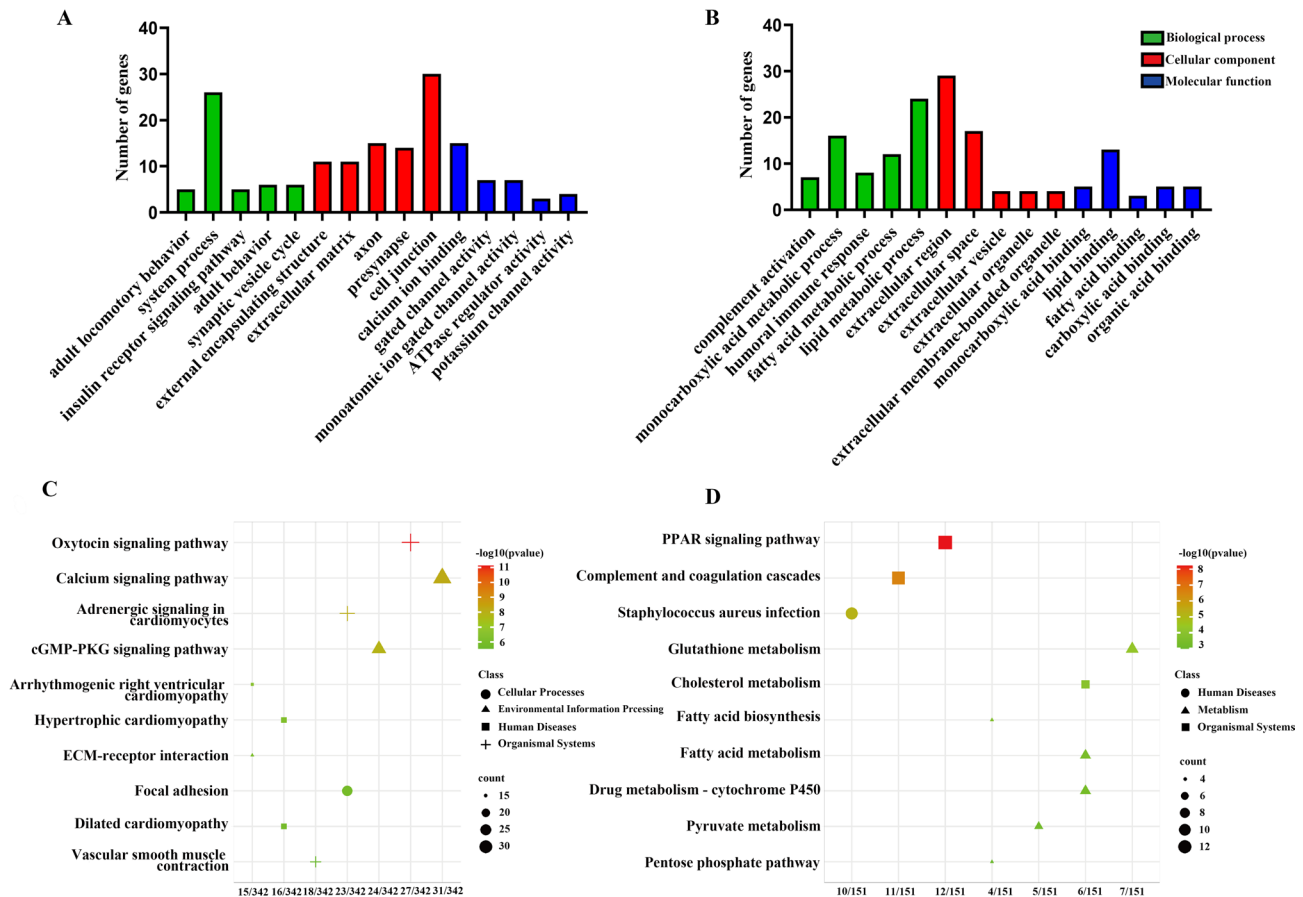


**Fig. 5** Gene ontology (GO) enrichment analysis and KEGG pathway analysis of genes differentially expressed between intramuscular fat (IMF) and subcutaneous fat (SF). **A** Top 5 biological processes, cellular components, and molecular functions enriched in genes upregulated in IMF compared to SF. **B** Top 5 biological processes, cellular components, and molecular functions enriched in genes downregulated in IMF compared to SF. **C** Top 10 KEGG pathways enriched in genes upregulated in IMF compared to SF. **D** Top 10 KEGG pathways enriched in genes downregulated in IMF compared to SF

Functional enrichment analyses of genes expressed at lower levels in IMF than SF indicated that many of these genes were enriched in the biological processes related to fatty acid biosynthesis and fatty acid binding. These results suggest that IMF has a lower capacity for *de novo* fatty acid synthesis and hence a lower capacity for providing fatty acids for triglyceride synthesis compared to SF, both of which may contribute to the slower growth of IMF compared to SF in cattle. During a brief (10 min) incubation with BODIPY FL C16 (a fluorescently labeled palmitate analog), IMF and SF explants accumulated similar levels of fluorescence, indicating that IMF and SF do not differ in long-chain fatty acid uptake. However, during an extended (4 h) incubation, SF explants accumulated significantly more fluorescence than IMF explants. These incubation data suggest that IMF has a lower capacity than SF for incorporating long-chain fatty acids into triglycerides or retaining them. The lower capacity for triglyceride synthesis in IMF than SF is consistent with the lower expression of *DGAT1* in IMF than SF because *DGAT1* plays a critical role in triglyceride

synthesis [67]. The lower capacity for retaining long-chain fatty acids in IMF than SF is consistent with the lower expression of *FABP4* in IMF than SF, as *FABP4* plays a crucial role in binding, transporting, and storing long-chain fatty acids in adipocytes [68]. While our transcriptomic data suggested that IMF may have a reduced capacity for *de novo* fatty acid synthesis compared to SF, this potential difference was not validated by functional assays measuring incorporation of radiolabeled acetate or glucose into lipids, which is one of the limitations of this study.

It is important to note that differences in gene expression and fatty acid binding between IMF and SF may also reflect differences in the developmental stage of these adipose depots. Adipocytes in IMF being smaller than those in SF may imply that IMF is at an earlier stage of development than SF [69]. Previous studies, such as those conducted in Japanese Black cattle, have shown that intramuscular adipocytes can reach much larger sizes than observed in the present study [70]. Therefore, some of the observed differences between IMF and SF may

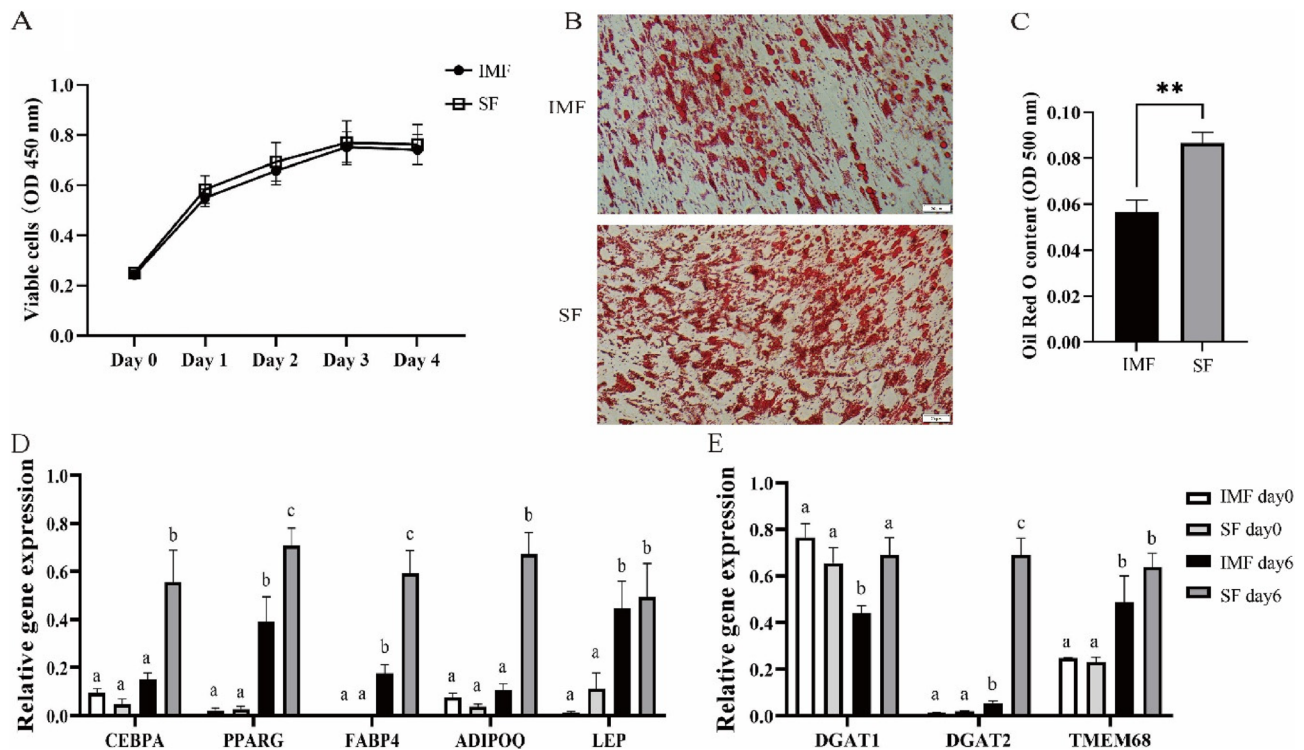


**Fig. 6** Comparing the abilities of stromal vascular fraction (SVF) cells of intramuscular fat (IMF) and subcutaneous fat (SF) to proliferate and differentiate into adipocytes. **A** Cell proliferation assessed using the CCK-8 assay. **B** Representative pictures of SVF cells stained with Oil Red O on day 6 of adipogenic differentiation. Scale bar: 20  $\mu$ m. **C** Quantity of Oil Red O extracted from cells stained with Oil Red O on day 6 of adipogenic differentiation. **\*\*** $P < 0.01$  ( $n = 6$ ). **D** Relative mRNA levels of selected adipocyte marker genes on day 0 (i.e., before differentiation) and day 6 of adipogenic differentiation. **E** Relative mRNA levels of 3 enzymes catalyzing triglyceride synthesis on day 0 and day 6 of adipogenic differentiation. Bars labeled with different letters are different within genes ( $P < 0.05$ ,  $n = 6$ )

reflect delayed development of IMF compared to SF. In addition, the unique microenvironment of IMF, which is embedded between muscle fibers, may influence its lipid metabolism and gene expression through paracrine signaling or physical constraints not present in subcutaneous fat [71]. The cell composition of IMF is different than that of SF, with the former containing muscle stem cells that are not present in SF and that are also capable of fatty acid uptake [72]. This cellular heterogeneity may lead to an underestimation of adipocyte-specific fatty acid uptake in IMF.

Pathway enrichment analyses of genes expressed at lower levels in IMF than SF revealed that some of these genes were involved in the PPAR signaling pathway. The PPARG protein is a master transcriptional regulator of adipogenesis [21]. Downregulation of the PPAR signaling pathway in IMF compared to SF suggests lower adipogenic activity in IMF, a finding supported by our experiments showing that SVF cells from IMF had lower adipogenic potential than those from SF. In support of this, gene expression analyses showed that several key adipocyte differentiation markers, including *CEBPA* and *PPARG* (adipogenic transcriptional regulators) [73], *FABP4* (a lipid chaperone) [74, 75], *ADIPOQ* and *LEP*

(adipocyte-specific hormones) [76–78], and *DGAT1*, *DGAT2*, and *TMEM68* (enzymes involved in triglyceride synthesis) [79–81], were all significantly induced during adipogenic differentiation, but most were expressed at lower levels in IMF-derived than to SF-derived SVF cells. Taken together, these results support the notion that slower differentiation of preadipocytes into adipocytes is another mechanism contributing to the delayed development and slower growth of IMF compared to SF in cattle.

Functional analyses of genes expressed at higher levels in IMF than in SF showed that these genes were enriched in the Wnt and oxytocin signaling pathways. The Wnt signaling pathway is a major pathway that inhibits the expression of *CEBPA* and *PPARG*, two critical transcriptional regulators of adipogenic differentiation [82, 83]. Upregulation of the Wnt signaling pathway in IMF compared to SF suggests that it may be one of the signaling pathways contributing to the lower adipogenic activity in IMF. Oxytocin has been recently shown to have lipolytic effects [84, 85]. Upregulation of the oxytocin signaling pathway in IMF compared to SF suggests that this may be another signaling pathway contributing to the delayed development and slower growth of IMF compared to SF in cattle.

Unlike terminally differentiated adipocytes, preadipocytes can proliferate [86]. The SVF of adipose tissue is rich in preadipocytes [87]. Our in vitro data showed that the SVF cells from intramuscular and subcutaneous fat did not differ in their proliferation rates. This result suggests that the significantly lower deposition of IMF compared to SF in cattle is not caused by slower proliferation of preadipocytes in IMF. Our histological data showed that mature adipocytes in IMF were significantly smaller than those in SF, and that IMF contained a higher proportion of smaller adipocytes compared to SF. These results are not only consistent with a previous study [88], but also align with our earlier findings that both the differentiation of preadipocytes into adipocytes and triglyceride synthesis are slower in IMF than in SF.

Many of the physiological differences between IMF and SF in cattle discussed above are inferred from differentially expressed mRNAs between the two adipose depots. An obvious limitation of this approach is that differentially expressed mRNAs do not always correspond to differentially expressed proteins [89], which are the primary functional units in cells. Therefore, the roles of genes, biological processes, and signaling pathways identified in this study in the delayed development and slower growth of IMF compared to SF in cattle remain to be further studied at the protein level.

## Conclusion

IMF may have lower fatty acid binding capacity, lower triglyceride synthesis, and lower adipogenic potential compared to SF in cattle. These potential differences help explain why the development and growth of IMF are delayed and slower compared to SF and why intramuscular adipocytes are smaller than subcutaneous adipocytes in cattle. These differences may be driven by the lower expression of genes like *AGPAT2*, *FABP4*, *ADIG*, *ADIRE*, *PLIN2*, and *PLIN5*, along with the higher expression of genes such as *FOXO6*, *SLC27A1*, *HDAC9*, *WWTR1*, and *PIK3C2A* in IMF. Additionally, these differences may arise from the reduced activation of the PPAR signaling pathway and the increased activation of the Wnt and oxytocin receptor signaling pathways in IMF compared to SF.

## Abbreviations

ABAM	antibiotics-antimicrobials
APC	adipose progenitor cell
BMP	bone morphogenetic protein
DAPI	4',6-diamidino-2-phenylindole
DEG	differentially expressed gene
DMEM	Dulbecco's modified eagle medium
FBS	fetal bovine serum
IMF	intramuscular fat
MSC	mesenchymal stem cell
PBS	phosphate buffered saline
qPCR	quantitative polymerase chain reaction
RNA-seq	RNA sequencing

SF	subcutaneous fat
SVF	stromal vascular fraction

## Supplementary Information

The online version contains supplementary material available at <https://doi.org/10.1186/s12864-025-11890-6>.

Supplementary Material 1.  
Supplementary Material 2.  
Supplementary Material 3.  
Supplementary Material 4.  
Supplementary Material 5.  
Supplementary Material 6.

## Acknowledgements

The authors would like to thank Smith Valley Meats (Rich Creek, VA, USA) for allowing us to take tissue samples from their cattle.

## Authors' contributions

Z.T. designed and conducted the experiments, analyzed the data, and wrote the manuscript. B.P. analyzed the data and wrote the manuscript. Z.Z. conducted the experiments and analyzed the data. H.J. conceived the study, designed the experiments, and revised the manuscript. All authors read and approved the final manuscript.

## Funding

This project was supported by the Agriculture and Food Research Initiative competitive grant 2021-67015-33398 from the USDA National Institute of Food and Agriculture.

## Data availability

The sequencing data from this study has been deposited in the NCBI GEO database (<https://www.ncbi.nlm.nih.gov/geo/>) under accession number GSE290253.

## Declarations

### Ethics approval and consent to participate

This study was conducted using bovine tissues collected at a commercial slaughterhouse. No live animals were directly involved in this study. According to the guidelines of the Institutional Animal Care and Use Committee (IACUC) of Virginia Tech, ethical approval was not required.

### Consent for publication

Not applicable.

### Competing interests

The authors declare no competing interests.

### Author details

<sup>1</sup>School of Animal Sciences, Virginia Tech, Blacksburg, VA 24061, USA

Received: 24 February 2025 / Accepted: 8 July 2025

Published online: 31 July 2025

## References

- Rosen ED, Spiegelman BM. What we talk about when we talk about fat. *Cell*. 2014;156(1–2):20–44.
- Moody WG, Cassens RG. A quantitative and morphological study of bovine longissimus fat cells. *J Food Sci*. 1968;33(1):47–52.
- Drouillard JS. Current situation and future trends for beef production in the United States of America - A review. *Asian-Australasian J Anim Sci*. 2018;31(7):1007–16.

4. Vernon RG. The growth and metabolism of adipocytes. In: Control and Manipulation of Animal Growth. Edited by Buttery PJ, Haynes, N.B. and Lindsay DB. Butterworths, London; 1986: 67–84.
5. Robelin J. Growth of adipose tissues in cattle - partitioning between depots, chemical-composition and cellularity - a review. *Livest Prod Sci.* 1986;14(4):349–64.
6. Sainz R, Hasting E. Simulation of the development of adipose tissue in beef cattle. In: Modelling nutrient utilization in farm animals. Cabi Wallingford UK; 2000: 175–82.
7. Cianzio DS, Topel DG, Whitehurst GB, Beitz DC, Self HL. Adipose tissue growth and cellularity: changes in bovine adipocyte size and number. *J Anim Sci.* 1985;60(4):970–6.
8. Pethick DW, Harper GS, Hocquette J-F, Wang Y. Marbling biology—what do we know about getting fat into muscle. *Proceedings of Australian beef—the leader! The Impact of Science on the Beef Industry.* Armidale: CRC for Beef Genetic Technologies; 2006. p. 103–10.
9. Li L, Zhu Y, Wang X, He Y, Cao B. Effects of different dietary energy and protein levels and sex on growth performance, carcass characteristics and meat quality of F1 Angus × Chinese Xiangxi yellow cattle. *J Anim Sci Biotechnol.* 2014;5(1):21.
10. Lau AM, Tseng YH, Schulz TJ. Adipogenic fate commitment of muscle-derived progenitor cells: isolation, culture, and differentiation. *Methods Mol Biology (Clifton NJ).* 2014;1213:229–43.
11. Zhang Y, Bellows CF, Kolonin MG. Adipose tissue-derived progenitor cells and cancer. *World J Stem Cells.* 2010;2(5):103–13.
12. Tan Z, Jiang H. Molecular and cellular mechanisms of intramuscular fat development and growth in cattle. *Int J Mol Sci.* 2024. <https://doi.org/10.3390/ijms25052520>.
13. Huang H, Song TJ, Li X, Hu L, He Q, Liu M, Lane MD, Tang QQ. BMP signaling pathway is required for commitment of C3H10T1/2 pluripotent stem cells to the adipocyte lineage. *Proc Natl Acad Sci U S A.* 2009;106(31):12670–5.
14. Gupta RK, Arany Z, Seale P, Mepani RJ, Ye L, Conroe HM, Roby YA, Kulaga H, Reed RR, Spiegelman BM. Transcriptional control of preadipocyte determination by Zfp423. *Nature.* 2010;464(7288):619–23.
15. Wu Z, Wang S. Role of kruppel-like transcription factors in adipogenesis. *Dev Biol.* 2013;373(2):235–43.
16. Deng K, Ren C, Liu Z, Gao X, Fan Y, Zhang G, Zhang Y, Ma ES, Wang F, You P. Characterization of RUNX1T1, an adipogenesis regulator in ovine preadipocyte differentiation. *Int J Mol Sci.* 2018;19(5): 1300.
17. Tong Q, Dalgin G, Xu H, Ting CN, Leiden JM, Hotamisligil GS. Function of GATA transcription factors in preadipocyte-adipocyte transition. *Science.* 2000;290(5489):134–8.
18. Wagoner B, Hausman DB, Harris RBS. Direct and indirect effects of leptin on preadipocyte proliferation and differentiation. *Am J Physiol Regul Integr Comp Physiol.* 2006;290(6):R1557–64.
19. Wabitsch M, Heinze E, Hauner H, Shymko RM, Teller WM, De Meyts P, Ilondo MM. Biological effects of human growth hormone in rat adipocyte precursor cells and newly differentiated adipocytes in primary culture. *Metabolism.* 1996;45(1):34–42.
20. Hausman DB, DiGirolamo M, Bartness TJ, Hausman GJ, Martin RJ. The biology of white adipocyte proliferation. *Obes Rev.* 2001;2(4):239–54.
21. Brun RP, Spiegelman BM. PPAR gamma and the molecular control of adipogenesis. *J Endocrinol.* 1997;155(2):217–8.
22. Bergan-Roller HE. Nutritional regulation of growth hormone-stimulated lipolysis. *Ph.D. United States -- North Dakota: North Dakota State University;* 2014.
23. Kersten S. Mechanisms of nutritional and hormonal regulation of lipogenesis. *EMBO Rep.* 2001;2(4):282–6.
24. Smith SB, Crouse JD. Relative contributions of acetate, lactate and glucose to lipogenesis in bovine intramuscular and subcutaneous adipose tissue. *J Nutr.* 1984;114(4):792–800.
25. Whitehurst GB, Beitz DC, Cianzio D, Topel DG. Fatty acid synthesis from lactate in growing cattle. *J Nutr.* 1981;111(8):1454–61.
26. Hood RL, Thornton RF. A technique to study the relationship between adipose cell size and lipogenesis in a heterogeneous population of adipose cells. *J Lipid Res.* 1980;21(8):1132–6.
27. Hudson NJ, Reverter A, Griffiths WJ, Yutuc E, Wang Y, Jeanes A, McWilliam S, Pethick DW, Greenwood PL. Gene expression identifies metabolic and functional differences between intramuscular and subcutaneous adipocytes in cattle. *BMC Genomics.* 2020;21(1):77.
28. Lee H-J, Jang M, Kim H, Kwak W, Park W, Hwang JY, Lee C-K, Jang GW, Park MN, Kim H-C, et al. Comparative transcriptome analysis of adipose tissues reveals that ECM-receptor interaction is involved in the depot-specific adipogenesis in cattle. *PLoS One.* 2013;8(6): e66267.
29. Schneider CA, Rasband WS, Eliceiri KW. NIH image to imageJ: 25 years of image analysis. *Nat Methods.* 2012;9(7):671–5.
30. Kolahi KS, Valent AM, Thornburg KL. Real-time microscopic assessment of fatty acid uptake kinetics in the human term placenta. *Placenta.* 2018;72–73:1–9.
31. Bolger AM, Lohse M, Usadel B. Trimmomatic: a flexible trimmer for illumina sequence data. *Bioinformatics.* 2014;30(15):2114–20.
32. Mortazavi A, Williams BA, McCue K, Schaeffer L, Wold B. Mapping and quantifying mammalian transcriptomes by RNA-seq. *Nat Methods.* 2008;5(7):621–8.
33. Pertea G. M P Pertea 2020 GFF utilities: GffRead and gffcompare. *F1000Res* 9 304–304.
34. Liao Y, Smyth GK, Shi W. Featurecounts: an efficient general purpose program for assigning sequence reads to genomic features. *Bioinformatics.* 2014;30(7):923–30.
35. Love MI, Huber W, Anders S. Moderated estimation of fold change and dispersion for RNA-seq data with DESeq2. *Genome Biol.* 2014;15(12):550.
36. Shannon P, Markiel A, Ozier O, Baliga NS, Wang JT, Ramage D, Amin N, Schwikowski B, Ideker T. Cytoscape: a software environment for integrated models of biomolecular interaction networks. *Genome Res.* 2003;13(11):2498–504.
37. Yu G, Wang LG, Han Y, He QY. Clusterprofiler: an R package for comparing biological themes among gene clusters. *OMICS.* 2012;16(5):284–7.
38. Ligasová A, Koberna K. Quantification of fixed adherent cells using a strong enhancer of the fluorescence of DNA dyes. *Sci Rep.* 2019;9(1):8701.
39. Livak KJ, Schmittgen TD. Analysis of relative gene expression data using real-time quantitative PCR and the 2(-Delta Delta C(T)) method. *Methods (San Diego Calif).* 2001;25(4):402–8.
40. Farmer SR. Regulation of PPARgamma activity during adipogenesis. *Int J Obes (Lond).* 2005;29(Suppl 1):S13–16.
41. Anton I, Kovács K, Holló G, Farkas V, Lehel L, Hajda Z, Zsolnai A. Effect of leptin, DGAT1 and TG gene polymorphisms on the intramuscular fat of Angus cattle in Hungary. *Livest Sci.* 2011;135(2):300–3.
42. Itabe H, Yamaguchi T, Nimura S, Sasabe N. Perilipins: a diversity of intracellular lipid droplet proteins. *Lipids Health Dis.* 2017;16(1):83.
43. Jones SF, Infante JR. Molecular pathways: fatty acid synthase. *Clin Cancer Res.* 2015;21(24):5434–8.
44. Sturdivant CA, Lunt DK, Smith GC, Smith SB. Fatty acid composition of subcutaneous and intramuscular adipose tissues and M. longissimus dorsi of Wagyu cattle. *Meat Sci.* 1992;32(4):449–58.
45. Campbell EMG, Sanders JO, Lunt DK, Gill CA, Taylor JF, Davis SK, Riley DG, Smith SB. Adiposity, lipogenesis, and fatty acid composition of subcutaneous and intramuscular adipose tissues of Brahman and Angus crossbred cattle. *J Anim Sci.* 2016;94(4):1415–25.
46. Zhang H, Dong X, Wang Z, Zhou A, Peng Q, Zou H, Xue B, Wang L. Dietary conjugated linoleic acids increase intramuscular fat deposition and decrease subcutaneous fat deposition in yellow breed × simmental cattle. *Anim Sci J.* 2016;87(4):517–24.
47. Abdalla BA, Chen X, Li K, Chen J, Yi Z, Zhang X, Li Z, Nie Q. Control of pre-adipocyte proliferation, apoptosis and early adipogenesis by the forkhead transcription factor FoxO6. *Life Sci.* 2021;265:118858.
48. Anderson CM, Stahl A. SLC27 fatty acid transport proteins. *Mol Aspects Med.* 2013;34(2):516–28.
49. Challa TD, Straub LG, Balaz M, Kiehlmann B, Donze O, Rudofsky G, Ukropec J, Ukropcova B, Wolfrum C. Regulation of de novo adipocyte differentiation through cross talk between adipocytes and preadipocytes. *Diabetes.* 2015;64(12):4075–87.
50. Qiu F, Xie L, Ma JE, Luo W, Zhang L, Chao Z, Chen S, Nie Q, Lin Z, Zhang X. Lower expression of *SLC27A1* enhances intramuscular fat deposition in chicken via down-regulated fatty acid oxidation mediated by *CPT1A*. *Front Physiol.* 2017;8:449.
51. Chatterjee TK, BJ E, Hui YK, SD W, HD Y, Weintraub NL. Role of histone deacetylase 9 in regulating adipogenic differentiation and high fat diet-induced metabolic disease. *Adipocyte.* 2014;3(4):333–8.
52. El Quarrat D, Isaac R, Lee YS, Oh DY, Wollam J, Lackey D, Riopel M, Bandyopadhyay G, Seo JB, Sampath-Kumar R, et al. TAZ is a negative regulator of PPARγ activity in adipocytes and TAZ deletion improves insulin sensitivity and glucose tolerance. *Cell Metabol.* 2020;31(1):162–e173165.
53. Alliouachene S, Bilanges B, Chaussade C, Pearce W, Foukas LC, Scudamore CL, Moniz LS, Vanhaesebroeck B. Inactivation of class II PI3K-C2α induces

- leptin resistance, age-dependent insulin resistance and obesity in male mice. *Diabetologia*. 2016;59(7):1503–12.
54. Cautivo KM, Lizama CO, Tapia PJ, Agarwal AK, Garg A, Horton JD, Cortés VA. AGPAT2 is essential for postnatal development and maintenance of white and brown adipose tissue. *Mol Metab*. 2016;5(7):491–505.
55. Fernández-Galilea M, Tapia P, Cautivo K, Morselli E, Cortés VA. AGPAT2 deficiency impairs adipogenic differentiation in primary cultured preadipocytes in a non-autophagy or apoptosis dependent mechanism. *Biochem Biophys Res Commun*. 2015;467(1):39–45.
56. Tontonoz P, Graves RA, Budavari AI, Erdjument-Bromage H, Lui M, Hu E, Tempst P, Spiegelman BM. Adipocyte-specific transcription factor ARF6 is a heterodimeric complex of two nuclear hormone receptors, PPAR gamma and RXR alpha. *Nucleic Acids Res*. 1994;22(25):5628–34.
57. Furuhashi M, Hotamisligil GS. Fatty acid-binding proteins: role in metabolic diseases and potential as drug targets. *Nat Rev Drug Discov*. 2008;7(6):489–503.
58. Wei S, Zan LS, Wang HB, Cheng G, Du M, Jiang Z, Hausman GJ, McFarland DC, Dodson MV. Adenovirus-mediated interference of *FABP4* regulates mRNA expression of *ADIPOQ*, *LEP* and *LEPR* in bovine adipocytes. *Genet Mol Res*. 2013;12(1):494–505.
59. Bahrami-Nejad Z, Zhang Z-B, Tholen S, Sharma S, Rabiee A, Zhao ML, Kraemer FB, Teruel MN. Early enforcement of cell identity by a functional component of the terminally differentiated state. *PLoS Biol*. 2022;20(12):e3001900.
60. Alvarez-Guaita A, Patel S, Lim K, Haider A, Dong L, Conway OJ, Ma MKL, Chiarugi D, Saudek V, O'Rahilly S, et al. Phenotypic characterization of *adig* null mice suggests roles for adipogenin in the regulation of fat mass accrual and leptin secretion. *Cell Rep*. 2021;34(10):108810.
61. Luna-Ramirez RI, Kelly AC, Anderson MJ, Bidwell CA, Goyal R, Limesand SW. Elevated norepinephrine stimulates adipocyte hyperplasia in ovine fetuses with placental insufficiency and IUGR. *Endocrinology*. 2023. <https://doi.org/10.1210/endo.2023-01177>.
62. Wang S, Liu J, Zhao W, Wang G, Gao S. Selection of candidate genes for differences in fat metabolism between cattle subcutaneous and perirenal adipose tissue based on RNA-seq. *Anim Biotechnol*. 2023;34(3):633–44.
63. Brasaemle DL, Rubin B, Harten IA, Gruia-Gray J, Kimmel AR, Londos C. Perilipin A increases triacylglycerol storage by decreasing the rate of triacylglycerol hydrolysis. *J Biol Chem*. 2000;275(49):38486–93.
64. Ramos SV, Turnbull PC, MacPherson REK. Adipose tissue depot specific differences of PLIN protein content in endurance trained rats. *Adipocyte*. 2016;5(2):212–23.
65. Li P, Wang Y, Zhang L, Ning Y, Zan L. The expression pattern of PLIN2 in differentiated adipocytes from Qinchuan cattle analysis of its protein structure and interaction with CGI-58. *Int J Mol Sci*. 2018;19(5):1336.
66. Wang H, Sreenivasan U, Hu H, Saladino A, Polster BM, Lund LM, Gong D-w, Stanley WC, Sztalryd C. Perilipin 5, a lipid droplet-associated protein, provides physical and metabolic linkage to mitochondria. *J Lipid Res*. 2011;52(12):2159–68.
67. Chitraju C, Walther TC, Farese RV. The triglyceride synthesis enzymes DGAT1 and DGAT2 have distinct and overlapping functions in adipocytes. *J Lipid Res*. 2019;60(6):1112–20.
68. Furuhashi M, Saitoh S, Shimamoto K, Miura T. Fatty acid-binding protein 4 (FABP4): pathophysiological insights and potent clinical biomarker of metabolic and cardiovascular diseases. *Clin Med Insights Cardiol*. 2014;8(Suppl 3):23–33.
69. Smith SB, Kawachi H, Choi CB, Choi CW, Wu G, Sawyer JE. Cellular regulation of bovine intramuscular adipose tissue development and composition. *J Anim Sci*. 2009;87(suppl14):E72–82.
70. Yamada T, Kamiya M, Higuchi M. Fat depot-specific effects of body fat distribution and adipocyte size on intramuscular fat accumulation in Wagyu cattle. *Anim Sci J*. 2020;91(1):e13449.
71. Kokta TA, Dodson MV, Gertler A, Hill RA. Intercellular signaling between adipose tissue and muscle tissue. *Domest Anim Endocrinol*. 2004;27(4):303–31.
72. Wang J, Li DL, Zheng LF, Ren S, Huang ZQ, Tao Y, Liu Z, Shang Y, Pang D, Guo H, et al. Dynamic palmitoylation of STX11 controls injury-induced fatty acid uptake to promote muscle regeneration. *Dev Cell*. 2024;59(3):384–e399385.
73. Avram MM, Avram AS, James WD. Subcutaneous fat in normal and diseased States 3. Adipogenesis: from stem cell to fat cell. *J Am Acad Dermatol*. 2007;56(3):472–92.
74. Thumser AE, Moore JB, Plant NJ. Fatty acid binding proteins: tissue-specific functions in health and disease. *Curr Opin Clin Nutr Metab Care*. 2014;17(2):124–9.
75. Trojnar M, Patro-Malysza J, Kimber-Trojnar Z, Leszczynska-Gorzela B, Mosiewicz J. Associations between fatty acid-binding protein 4-A Proinflammatory adipokine and insulin resistance, gestational and type 2 diabetes mellitus. *Cells*. 2019;8(3):227.
76. Hu E, Liang P, Spiegelman BM. AdipoQ is a novel adipose-specific gene dysregulated in obesity. *J Biol Chem*. 1996;271(18):10697–703.
77. Foucan L, Maimaitiming S, Larifla L, Hedreville S, Deloumeaux J, Joannes MO, Blanchet-Deverly A, Velayoudom-Céphise FL, Aubert R, Salamon R, et al. Adiponectin gene variants, adiponectin isoforms and cardiometabolic risk in type 2 diabetic patients. *J Diabetes Invest*. 2014;5(2):192–8.
78. Havel PJ. Role of adipose tissue in body-weight regulation: mechanisms regulating leptin production and energy balance. *Proc Nutr Soc*. 2000;59(3):359–71.
79. Yen CL, Stone SJ, Koliwad S, Harris C, Farese RV Jr. Thematic review series: glycerolipids. DGAT enzymes and triacylglycerol biosynthesis. *J Lipid Res*. 2008;49(11):2283–301.
80. Wang Y, Zeng F, Zhao Z, He L, He X, Pang H, Huang F, Chang P. Transmembrane protein 68 functions as an MGAT and DGAT enzyme for triacylglycerol biosynthesis. *Int J Mol Sci*. 2023;24(3):2012.
81. McLelland G-L, Lopez-Osias M, Verzijl CRC, Ellenbroek BD, Oliveira RA, Boon NJ, Dekker M, van den Hengel LG, Ali R, Janssen H, et al. Identification of an alternative triglyceride biosynthesis pathway. *Nature*. 2023;621(7977):171–8.
82. Prestwich TC, Macdougald OA. Wnt/beta-catenin signaling in adipogenesis and metabolism. *Curr Opin Cell Biol*. 2007;19(6):612–7.
83. Longo KA, Wright WS, Kang S, Gerin I, Chiang SH, Lucas PC, Opp MR, MacDougald OA. Wnt10b inhibits development of white and brown adipose tissues. *J Biol Chem*. 2004;279(34):35503–9.
84. Assinder SJ, Boumelhem BB. Oxytocin stimulates lipolysis, prostaglandin E2 synthesis, and leptin secretion in 3T3-L1 adipocytes. *Mol Cell Endocrinol*. 2021;534:111381.
85. Li E, Wang L, Wang D, Chi J, Lin Z, Smith GI, Klein S, Cohen P, Rosen ED. Control of lipolysis by a population of oxytocinergic sympathetic neurons. *Nature*. 2024;625(7993):175–80.
86. Sajic T, Ferreira Gomes CK, Gasser M, Caputo T, Bararpour N, Landaluze-Iturriria E, Augsburg M, Walter N, Hainard A, Lopez-Mejia IC, et al. SMYD3: a new regulator of adipocyte precursor proliferation at the early steps of differentiation. *Int J Obes*. 2024;48(4):557–66.
87. Farrar JS, Martin RK. Isolation of the stromal vascular fraction from adipose tissue and subsequent differentiation into white or beige adipocytes. *Methods Mol Biology (Clifton NJ)*. 2022;2455:103–15.
88. Gardan D, Gondret F, Louveau I. Lipid metabolism and secretory function of porcine intramuscular adipocytes compared with subcutaneous and perirenal adipocytes. *Am J Physiol Endocrinol Metab*. 2006;291(2):E372–380.
89. Koussounadis A, Langdon SP, Um IH, Harrison DJ, Smith VA. Relationship between differentially expressed mRNA and mRNA-protein correlations in a xenograft model system. *Sci Rep*. 2015;5(1):10775.

## Publisher's Note

Springer Nature remains neutral with regard to jurisdictional claims in published maps and institutional affiliations.